

Article

Microfluidic sensors platform technology to enhancement fluorescence

Noor luay Hussein, Zainab Al-Bawi

Institute of Laser for Postgraduate Studies, University of Baghdad, Baghdad, Iraq

*Correspondence: nour.loaiy1101a@ilps.uobaghdad.edu.iq, nour.loaiy1101a@ilps.uobaghdad.edu.iq, zainab@ilps.uobaghdad.edu.iq

Available from: <http://dx.doi.org/10.21931/RB/CSS/2023.08.03.52>

Abstract

The integrated concepts of biology, physics, fluid dynamics, chemistry, material science, and microelectronics provide the foundation of the relatively young area of microfluidics. Various materials may be processed into tiny chips with microscale channels and chambers. Regarding PMMA material and production methods, microfluidic biosensor platform technology also focuses on enhancing rhodamine B's fluorescence via adding carbon nanotubes, with additional benefits including restricted detection, high sensitivity, high stability, repeatability., quick response analysis, low consumption of sample volume, high throughput, also ease of operation applications of these remarkable devices.

Keywords: microfluidics, CO2 laser ablation; Confocal Laser Scanning Microscope, PMMA, Carbon nanotubes, fluorescent.

Introduction

The capacity to accurately construct micron-to-nanoscale architecture to influence the physical and chemical environments is provided via microfluidic technology 1. In the relatively new discipline of microfluidics, fluid control and manipulation in tightly limited channels, chambers, and chips are the subjects of this research. Since they were first developed, microfluidic chips have found applications in various sectors, including molecular biology and the continuous manufacture of chemicals—investigating pharmaceuticals in vitro and mimicking various organs. The minimal amount of fluids needed and the microfluidic chips' excellent mobility and relatively cheap cost make them of tremendous interest and have a wide range of applications. The advantages of mobility, accuracy, speed, and minimal sample volumes make this technology a game-changer compared to traditional laboratory analysis and diagnosis. Microfluidic technology has been widely researched and used in biology, medicine, food, agriculture, and the environment 2. Microfluidic devices can potentially reduce the risk of biohazards and are therefore suitable for use in public and environmental health microbiology contexts 3. Cells are analyzed within a closed system, and the devices are rapidly sterilized after each use, so these factors combine to make the devices acceptable for use. One of the primary problems of the microfluidic chip is that it is challenging to mix fluids inside the chip because of its small size and low flow rates. In addition, restricting liquids to the relatively tiny quantities typical with microfluidic chips could result in several adverse impacts. 2,4. The production of polymer-based microfluidic devices now primarily uses poly (methyl methacrylate) (PMMA) polymer 5,6. In our technology, the design is created using AutoCAD, and the plexiglass (PMMA) slab is

machined using a CO₂ laser in a one-touch automated procedure. This is this method's most significant benefit since it allows for the manufacturing of an infinite number of microchannels from a single mold without having to repeat the machining procedure. A representational illustration of our production process is shown in Fig. 1. PMMA microchannels, the principal material for microfluidics, are provided via the process, ensuring the constant manufacture of identical channels with flawlessly reproducible outcomes ⁷. Several research teams have recently reported using the fluorescence detection approach with microfluidic systems. The simplicity, cheap cost, excellent sensitivity, high selectivity, and suitability for on-site and real-time signaling have made the fluorescence detection approach more practical. The concentration of the analytes in intact biosamples may also be determined using the fluorescence detection technique light-induced fluorescence (LIF). Fluorescence-based sensors have gained popularity among the many optical-chemical techniques because of their quick reaction times, low equipment needs, and affordable price. These techniques are based on a change in an optically active molecular indicator's fluorescence intensity in response to a concentration and low detection limit ^{8,9}. Rhodamine derivatives have been used significantly as fluorescent or colorimetric chemosensors to distinguish between various metal ions. Because of their strong dependence on these dramatic changes, rhodamine derivatives have been used successfully as ion-selective chemosensors. This is possible thanks to the combination of their relatively long emission wavelengths, which have demonstrated significant advantages in fluorescence detection ¹⁰⁻¹⁴. However, since only very tiny quantities of samples are used for fluorescence detection in microfluidic chips, the fluorescence intensity is often very low. This has the unavoidable effect of lowering both the detection limit and the test's sensitivity. Because of this, the development of a portable fluorescence-enhanced sensor is essential to increase the sensitivity of biomaterial detection via carbon nanotubes. The combination of a microfluidic sensing system with a light-induced fluorescence (LIF) detection setup and an optical fiber utilized to collect the signal and transport it to a spectrometer device is shown in this study.

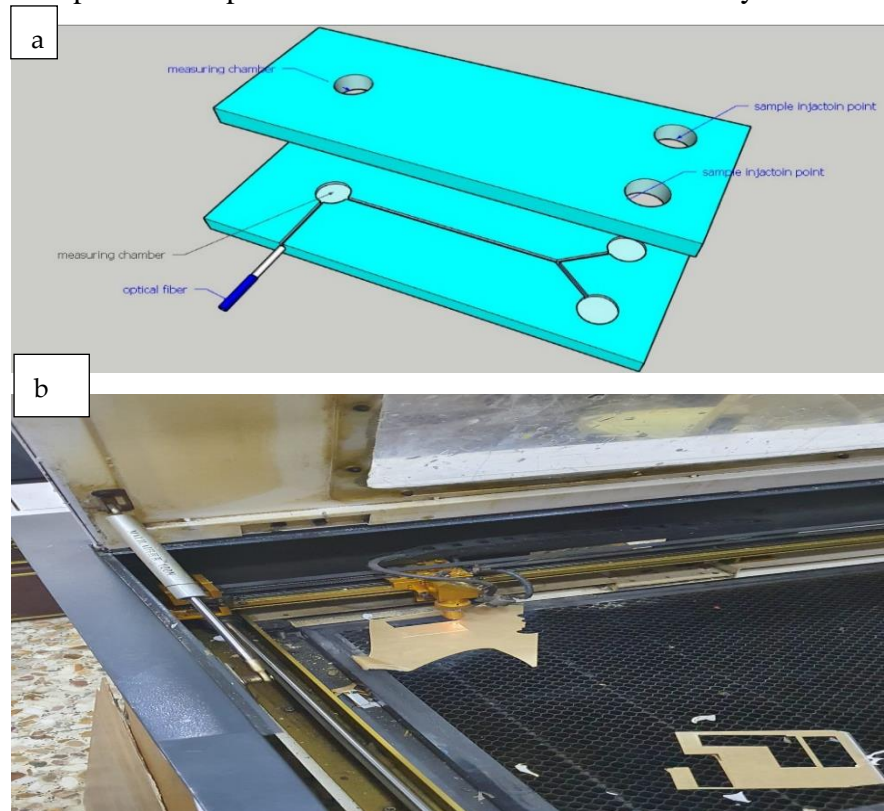


Fig. (1). (a) Design of the microfluidic sensor system schematic illustration. Making of the microfluidic sensor system (option b).

Materials and Methods

Fabrication of Microfluidic Devices

Microfluidic Device Materials

Choosing the best material for device manufacturing is one of the critical tasks in microfluidic applications. When selecting the material, it is necessary to consider many other crucial properties, including its durability, ease of fabrication, transparency, biocompatibility, chemical compatibility with the implied reagents, fulfillment of the reaction's temperature and pressure requirements, and the potential for surface functionalization. 15.

Acrylic polymer (C₅H₈O₂) PMMA is employed in the current study. The samples were cut into rectangular forms with straight channels (Y shapes) and dimensions of (19492.5) mm. They were then cleaned in water to eliminate surface contaminants and keep the microchannel surfaces defect-free and smooth. The research has considered various laser factors, including power scan speed and their impact on the depth, breadth, and surface roughness of the process's end result. PMMA samples with a thickness of 2.5 mm were employed, and a CO₂ laser was used as the laser source (Jumei Acrylic Manufacturing, Shanghai, China). According to the results of our research, a flawless surface finish for microchannels may be achieved with a CO₂ laser with less effort overall. Throughout this research, we looked at the samples' cutting surface form and surface roughness. Prior to that, AUTOCAD software was used to create the microfluidic chip's profile (Version 23.0, Autodesk, Inc., San Rafael, CA, USA). Finally, the PMMA-Chloroform-PMMA structure was squeezed using a finger in a few minutes to speed up bonding and close off the created microchannels. The manufacturing process was completed by connecting the pipes for the inlets and outflow ports to the holes of the syringe pump (Perfusor Compact, China)—microfluidic chips.

Laser-Based Processes

Although lasers are often costly instruments, they are seen as a more accessible manufacturing approach when compared to cleanroom facility expenditures. Furthermore, without the risks associated with chemical production techniques, laser ablation enables the quick and flexible synthesis of microfluidic patterns on various materials. Lasers' primary operating mechanism is the stimulated emission of electromagnetic radiation, which optically amplifies light. The thermal deterioration effect engraves the surface of the working material by creating a microstructure. In greater detail, the chemical bonds that hold polymer molecules together are broken via short-duration laser pulses of specified wavelengths, and the rapidly rising temperature and pressure that follow cause decomposed polymer fragments to be ejected. A photo-ablated cavity is thus created. The disadvantages of this technology include low throughput, unfavorable surface effects, weak repeatability due to inadequate laser focusing control, and product quality differences between various laser types 15,16. In order to laser engrave also cut polymer, a (60)W model of a continuous wave (CW) CO₂ laser, computer numerically controlled (CNC) cutting system (LiaochengJK-4060, Laser Engraving Cutting, Machine, China). Table 1 contains the specifics of the process parameters used so that this inquiry could produce its conclusions. Laser parameters such as power (20, 40) W and (250, 350, 500) mm/s scan speeds were modified. Microscopes were used to measure the microfluidic chips' distinctive size and shape: Amscope, United States, 5X-180X Manufacturing Zoom Stereo Microscope with 144-LED Ring Light and 10MP Digital Camera. The magnifying powers offered via this microscope include (5X)—the depth and roughness of the microfluidic chips with a laser confocal microscope in (Iran).

Optical fiber integration in microfluidic sensor

All optical fibers had their outer protective and jacket layers removed, leaving just the core and cladding layer. Stripped fibers were sliced using a fiber scribe to create a flat surface at the fiber tip end. By using microscopic imaging, the flatness at the fiber ends was validated. Under careful inspection with a digital microscope, optical fibers were manually put into the chip via the corresponding fiber guide structures; they were then secured to the PMMA slide with a channel. (FT800UMT, Multimode Fiber, 0.39 NA, Low OH, 800 m Core, Thorlabs) Detection Fibers The Spectrometer receives fluorescence light (excitation laser ND-YAG 532 nm using technique LIF) captured via a detector fiber.

Light gathered via the detection fiber is attached to Temporary connections (830 mFC/PC connectors, MM stainless-steel Ferrule, Thorlabs) to detect transmitted light. To a Compact CCD Spectrometer (CCS200 - Compact Spectrometer, Extended Range: 200 - 1000 nm, Thorlabs), fluorescence light is gathered via a detector fiber.

Results

Effect Scans speed and power of laser CO₂

Modifying the speed and power settings at a fixed frequency (500 Hz) and altering the speed and power settings, the amount of energy given via the laser may be fine-tuned by using inside the designs created using the Corel DRAW program. The use of various settings for both speed and power made this accomplishment attainable. In Figure 2, microscope photos of a sample of microfluidic channel engravings are displayed, with graphical data indicating variations in etched depth as a function of scan speed for a particular power level. These data indicate how the depth of the engraving varies as a function of the scan speed. Even though the laser's power was only 40 W and the scan speed was (250,350,500 mm/s), the engraving's maximum width and depth measured 173.66 μ m and 92.678 μ m, respectively, while the engraving's minimum width and depth measured around 146.66 μ m also 89.951 μ m. These findings are shown in the Figure (5). Suppose the relatively high PMMA material removed from the surface needs to be adequately pushed away via convective forces from the local temperature hotspot. In that case, it will re-solidify chaotically on the engraved surface, resulting in occasional unevenness in the engraving depth. This can be avoided by ensuring that the convective forces from the hotspot are strong enough.

The laser spot radius, which for the system that was used was approximately 114.66 micrometers, was the limiting factor in terms of the minimum width of a channel that could be generated via the system through the use of a single engraving pass. This was because the laser spot radius was smaller than the minimum width of a channel that could be generated. Larger channel widths could be easily formed by increasing the width of the designs in the Corel DRAW program Illustrator, which is then translated to raster scans of the laser alongside the origin path until the desired channel width is engraved. This process could be repeated as many times as necessary until the desired width of the channel was engraved. It was possible to repeat this operation several times in order to engrave the channel to the appropriate width. Citation needed: The bulk of the increase in average roughness may be attributed to the micro-trenches. As the power is increased to accomplish a deeper engraving, the size of the formed grooves also rises to accommodate the additional depth. As was said before, the laser can convert a specific pattern into either an engraved pattern or a cut pattern, depending on the requirements of the particular design. Throughout the engraving process, adjusting the parameters of the laser to allow for additional customization of the amount of power provided via the laser is possible. As can be seen in Table, there is a pattern that resembles a linear trend in the change in the value of (engraved depth -width), which was found for modifications in the parameters of the laser. This trend was seen in general.

Also, it is shown here in Table for your perusal (1). Ultimately, the settings for a laser with a higher power could be fine-tuned to permit the development of deeper depths and bigger channels. This was a significant breakthrough.

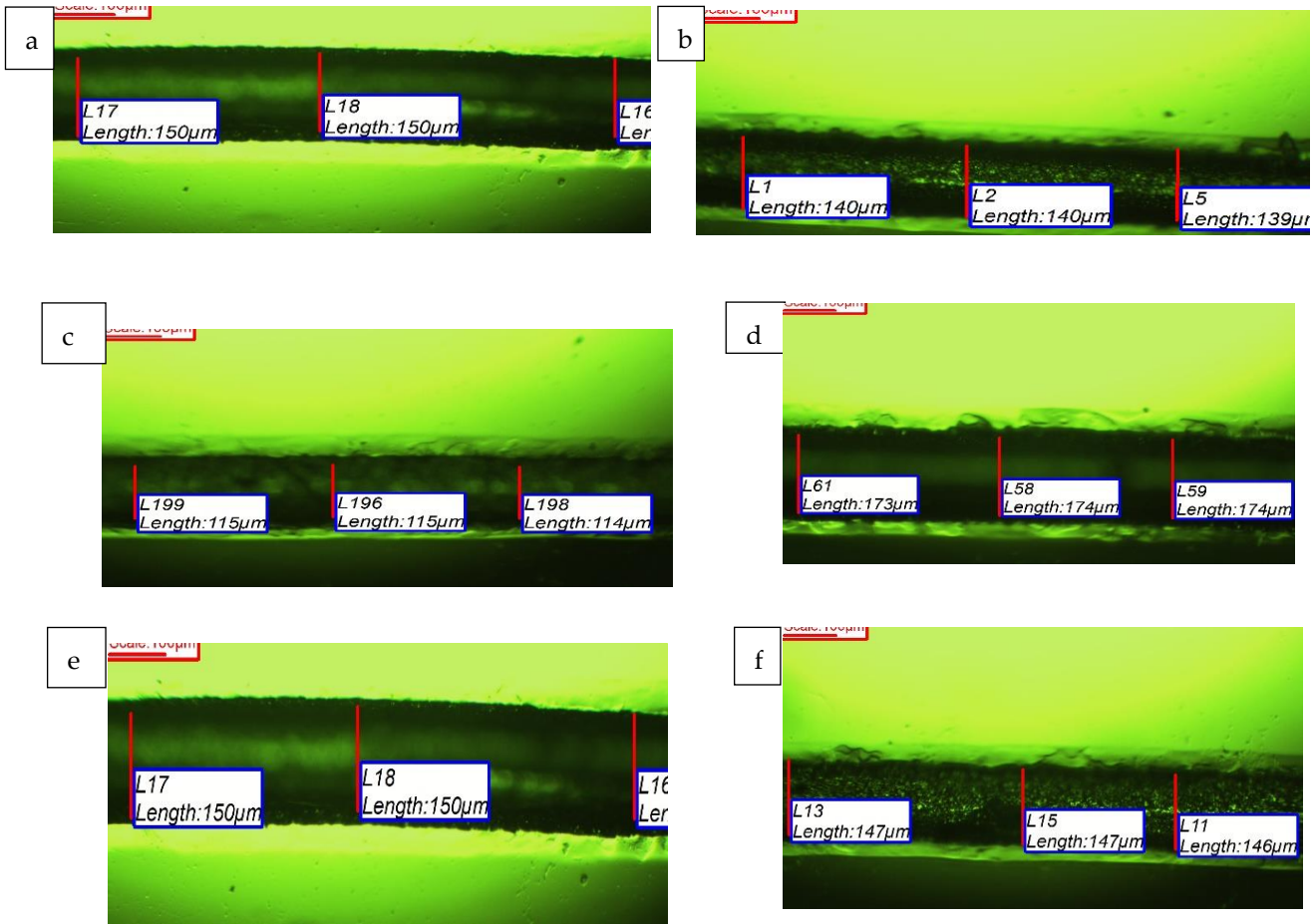
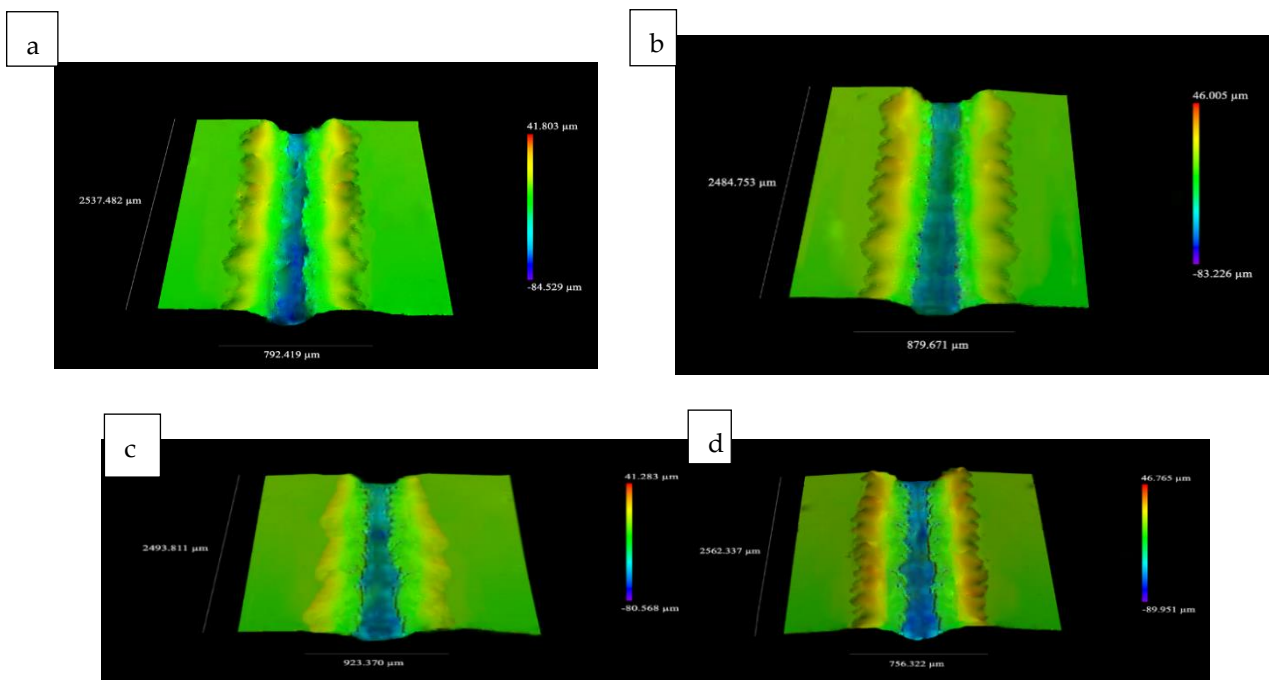


Fig.(2). Showing the width of the microfluidic chips via the optical microscope images velocity of laser is t at 250,350,500 mm/s a,b,c) power 20 w, d,e,f) power 40 w.



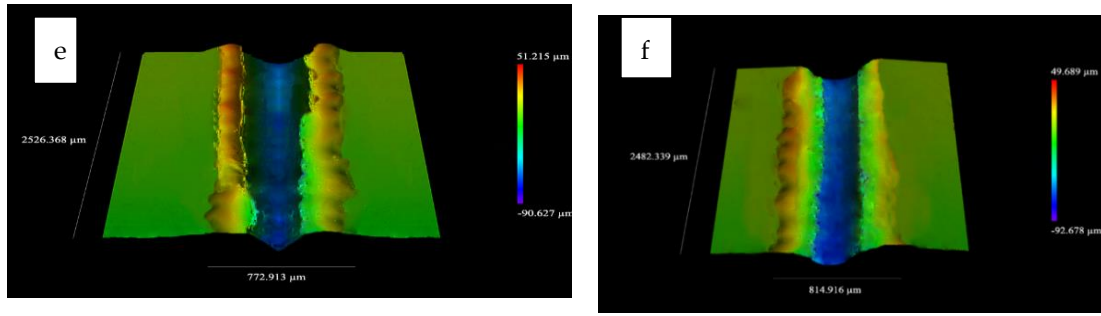


Fig.(3). Showing the depth of the microfluidic chips via Confocal Laser Scanning Microscope a,b,c) power 20 w at scan speed (250,350,500 mm/s), d,e,f) power 40 w at scan speeds (250,350,500 mm/s).

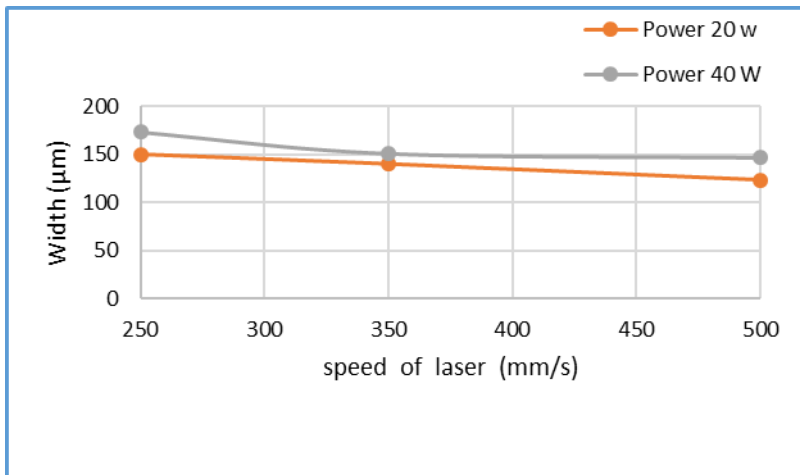


Fig.(4). Measurement of PMMA microchannel characteristics at various speeds. The laser-machined microchannel's Y straight-line microchannel.

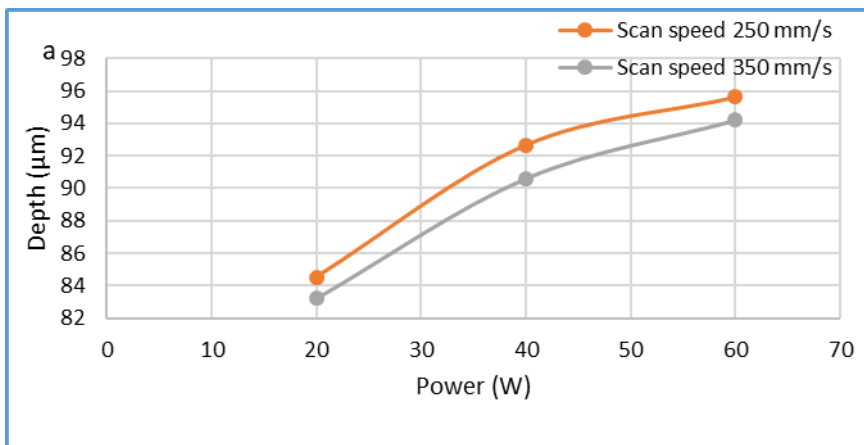


Fig.(5). depth of the microfluidic chips via Confocal Laser Scanning Microscope depth at the power of laser 20,40 W.

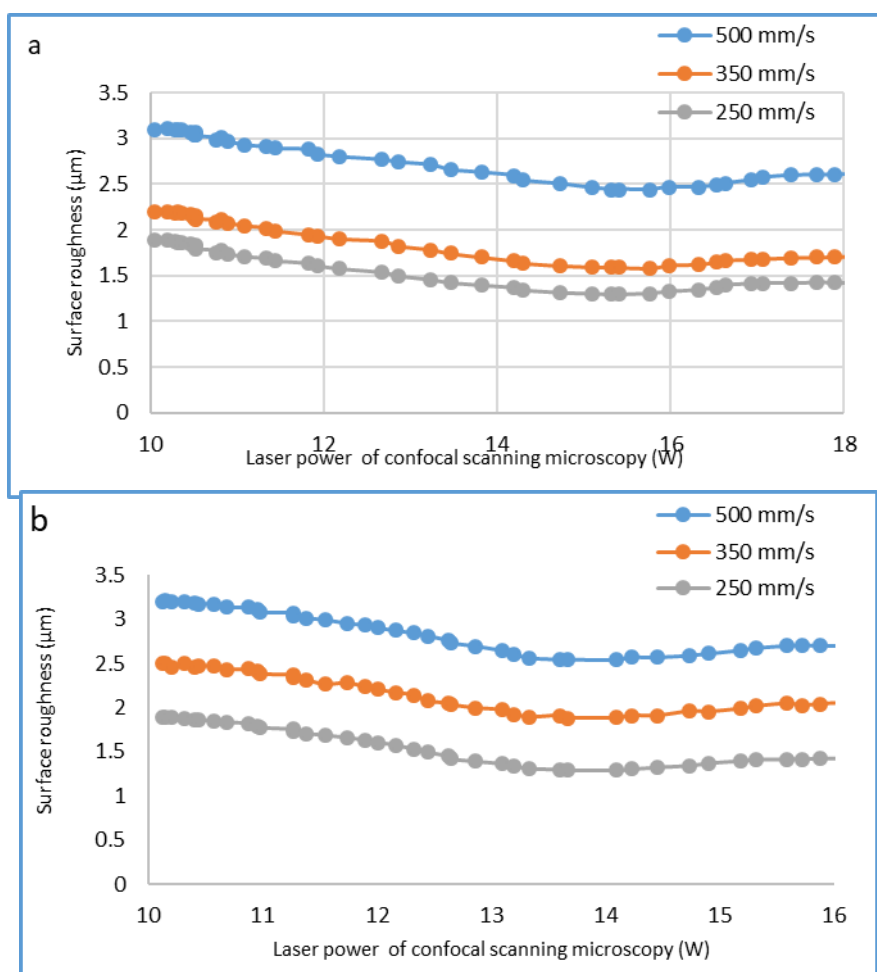


Fig.(6). Showing the Surface roughness of the optical fiber microfluidic chips via Confocal Laser Scanning Microscope a,b,c) at power (20,40) W straight channels.

Fluorometric Characterizations of Rhodamine B

The other optical solid biosensor that identifies analytes also offers excellent sensitivity and specificity in target identification fluorescence. An emission fiber is used to collect the fluorescence signal that is released via fluorescent dyes. Also, a spectrometer is used to detect the signal. After producing droplets with varying Rhodamine B concentrations, the researchers examined the levels of fluorescence emitted via the samples. The shift in wavelength was caused by a linear rise in fluorescence intensity due to increased dye concentration. The detector has a dynamic range extending from 100 mg/l to 3.125 mg/l. The fluorometric property of Rhodamine B in lower concentrations was studied in deionized (DI) water. This can be seen as the fluorescent halo. The dye's fluorescence can diffuse more profoundly into the PMMA microfluidic sensor at (power 40 W, scan speed 250 mm/s) with the RhB solution flowing continually in the microchannel. This can be seen as wider fluorescent bands, with each high concentration having a higher intensity. Adding 1.5625–6.25 mg/l of carbon nanotubes (CNTs) may enhance a lower concentration of Rhodamine B at 3.125 mg/l. This can be observed in Table (2).

Discussion

Additionally, the scan's speed affects the engraving's depth, as seen in Figure 2. Several settings were used (see Figure) to evaluate the laser's capacity for repeatability concerning engraving channels with varied depths 3. As can be observed, reducing the speed rate increased the amount of time spent interacting with the PMMA substrate, resulting in the development of deeper and broader channels. It was determined that a laser with a fixed power of 20 W could achieve a minimum engraving width and depth of roughly 114.66 2,80.568 m and a maximum engraving width and depth of nearly 150 m 2, 84.529 m. On the other hand, the laser's scan speed could be altered (see Fig.). The laser beam's intensity must be modified to do this 4.

It was determined that the average roughness rose together with the channel width and engraving depth, as shown in Figure. This was one of the findings that emerged from the research 6. Variations in convective material ejection are responsible for the increased production of residual polymer residues, increasing surface roughness. This phenomenon may be explained. This issue is accentuated with greater power (that is, while producing deeper channels) due to the micro-trenches generated via raster scanning and the Gaussian power distribution of the laser 17.

18 The constructed apparatus was tested to see how well it could detect fluorescence. Rhodamine B was used as a reference dye to characterize the fluorescence measurement. A microfluidic chip has an excitation fiber that is linked to a laser also embedded within the chip

These findings demonstrate that the created setup is compatible with conducting high-efficiency fluorescence measurements in various analytical and biochemical applications; they agree with 19,20.

Conclusion

In this study, we presented a microfluidic biosensor for establishing a multi-parametric measuring system via integrating optical fibers and PMMA into the biosensor's design. In order to measure fluorescence parameters, optical fiber was inserted at an orthogonal angle. The fluorescence values that were obtained served as concentration parameters. Because of the hydrophobic nature of Rhodamine B, it was chosen to serve as a model drug in the research conducted on the absorption of small molecules into PMMA microfluidic biosensors. When the RhB solution came into contact with the PMMA walls of the microchannel, it was noticed that the dye diffused into the PMMA. The intensity could be quantified using fluorescence microscopy. Also, it was discovered to closely follow the Fickian diffusion rules, which rendered the behavior constant also predictable. These areas near the channel walls operate as a reservoir for the dye. The diffusion of the dye into the matrix is at its greatest when it is at its lowest concentration. Also, it tends to slow down as it passes through lower concentrations. The release of molecules after being put into the PMMA microfluidic biosensor might be studied using this behavior.

Acknowledgements

The authors express our heartfelt appreciation and gratitude to everyone who helped complete this study, particularly the Research Review Committee. The Institute of Laser for Postgraduate Studies at the University of Baghdad funded the study.

References

1. Holloway, Paul M., et al. "Advances in microfluidic in vitro systems for neurological disease modeling." *Journal of Neuroscience Research* 99.5 ; **2021**: 1276-1307.
2. Gao, Yuefeng, et al. "Fluorescence-enhanced microfluidic sensor for highly sensitive in-situ detection of copper ions in lubricating oil." *Materials & Design* 191 (**2020**): 108693.
3. Yamaguchi, Nobuyasu, et al. "Rapid on-site monitoring of Legionella pneumophila in cooling tower water using a portable microfluidic system." *Scientific Reports* 7.1 (**2017**): 1-8.
4. Workamp, Marcel, Vittorio Saggiomo, also Joshua A. Dijkman. "A simple low pressure drop suspension-based microfluidic mixer." *Journal of Micromechanics also Microengineering* 25.9 (**2015**): 094003.
5. Mohammed, Mazher I., et al. "Fabrication of microfluidic devices: Improvement of surface quality of CO₂ laser machined poly (methylmethacrylate) polymer." *Journal of micromechanics also microengineering* 27.1 (**2016**): 015021.
6. Alshrefi, Saif M., et al. "Effect of 532 nm KTP Nd: Yag Laser on Poly Methyl Methacrylate Polymer Optical Properties." *NeuroQuantology: An Interdisciplinary Journal of Neuroscience also Quantum Physics*, vol. 18, no. 2, Feb. 2020, pp. 133+. Gale Academic One-File, link.gale.com/apps/doc/A676650093/AONE?u=anon~b2686782&sid=google-scholar&xid=10ecd616. Accessed 7 Aug. **2022**.
7. Guler, Mustafa Tahsin, Murat Inal, also Ismail Bilican. "CO₂ laser machining for microfluidics mold fabrication from PMMA with applications on viscoelastic focusing, electrospun nanofiber production, also droplet generation." *Journal of Industrial and Engineering Chemistry* 98 (**2021**): 340-349.
8. Moradi, Vahid, Mohsen Akbari, also Peter Wild. "A fluorescence-based pH sensor with microfluidic mixing also fiber optic detection for wide range pH measurements." *Sensors also Actuators A: Physical* 297 (**2019**): 111507.
9. Kim, Ha Na, et al. "Rhodamine hydrazone derivatives as Hg²⁺ selective fluorescent also colorimetric chemosensors also their applications to bioimaging also microfluidic system." *Analyst* 136.7 (**2011**): 1339-1343.
10. Liu, Chuantao, et al. "Rhodamine based turn-on fluorescent sensor for Hg²⁺ also its application of microfluidic system also bioimaging." *Tetrahedron* 73.34 (**2017**): 5189-5193.
11. Abdulkareem, E. A., Abdulsattar, J. O., & Abdulsattar, B. O. Iron (II) Determination in Lipstick Samples using Spectrophotometric also Microfluidic Paper-based Analytical Device (μPADs) Platform via Complexation Reaction with Iron Chelator 1, 10-phenanthroline: A Comparative Study. *Baghdad Science Journal*, **2022**; 19(2), 0355-0355.
12. Alraziqi, Z. N. R., & Mansoor, H. S. Experimental Investigation for Some Properties of PMMA Denture Base Strengthened via Different Nanoadditives. *Iraqi Journal of Science*, **2020**;2913-2925.
13. Iyer, M. Adiraj, also D. T. Eddington. "Storing also releasing rhodamine as a model hydrophobic compound in polydimethylsiloxane microfluidic devices." *Lab on a Chip* 19.4 (**2019**): 574-579.
14. Huang, Weikun, et al. "A Multiplexed Microfluidic Platform toward Interrogating Endocrine Function: Simultaneous Sensing of Extracellular Ca²⁺ also Hormone." *ACS Sensors* 5.2 (**2020**): 490-499.
15. Niculescu, Adelina-Gabriela, et al. "Fabrication also applications of microfluidic devices: A review." *International Journal of Molecular Sciences* 22.4 (2021): **2011**.
16. Shehab, Abeer A., et al. "Hole characteristic of CO₂ laser drilling of poly-methyl methacrylate PMMA." *Journal of Mechanical Engineering Research also Developments* 43.3 (**2020**): 186-197.
17. Mohammed, Mazher I., et al. "Fabrication of microfluidic devices: Improvement of surface quality of CO₂ laser machined poly (methylmethacrylate) polymer." *Journal of micromechanics also microengineering* 27.1 (**2016**): 015021.
18. Wang, Jing, Yong Ren, also Bei Zhang. "Application of microfluidics in biosensors." *Advances in Microfluidic Technologies for Energy and Environmental Applications* (**2020**).
19. Hengoju, S., et al. "Optofluidic detection setup for multi-parametric analysis of microbiological samples in droplets." *Biomicrofluidics* 14.2 (**2020**): 024109.
20. Hussein, Noor Luay, et al. "Simulation of Optical Energy Gap for Synthesis Carbon Quantum Dot via Laser Ablation." *Iraqi Journal of Science* (**2019**): 52-56.

Received: May 15, 2023/ Accepted: June 10, 2023 / Published: June 15, 2023

Citation: Hussein, N.L.; Al-Bawi , Z. Microfluidic sensors platform technology to enhancement fluorescenceRevis Bionatura 2023;8 (3) 52. <http://dx.doi.org/10.21931/RB/CSS/2023.08.03.52>